

# Tracking Temperature Dependent Relaxation Times of Individual Ferritin Nanomagnets with a Wide-band Quantum Spectrometer

Eike Schäfer-Nolte,<sup>1,2</sup> Lukas Schlipf,<sup>1,2</sup> Markus Ternes,<sup>1,\*</sup>  
Friedemann Reinhard,<sup>2</sup> Klaus Kern,<sup>1,3</sup> and Jörg Wrachtrup<sup>2,1</sup>

<sup>1</sup>Max-Planck Institute for Solid State Research, 70569 Stuttgart, Germany

<sup>2</sup>3rd Institute of Physics and Research Center SCoPE, University Stuttgart, 70569 Stuttgart, Germany

<sup>3</sup>Institut de Physique de la Matière Condensée, École Polytechnique Fédérale de Lausanne, 1015 Lausanne, Switzerland

(Dated: June 3, 2014)

We demonstrate the tracking of the spin dynamics of ensemble and individual magnetic ferritin proteins from cryogenic up to room temperature using the nitrogen-vacancy color center in diamond as magnetic sensor. We employ different detection protocols to probe the influence of the ferritin nanomagnets on the longitudinal and transverse relaxation of the nitrogen-vacancy center, which enables magnetic sensing over a wide frequency range from Hz to GHz. The temperature dependence of the observed spectral features can be well understood by the thermally induced magnetization reversals of the ferritin and enables the determination of the anisotropy barrier of single ferritin molecules.

PACS numbers: 75.75.Jn, 76.30.Mi

The study of magnetic fluctuations – time-dependent deviations of a magnetic system from equilibrium – is of high intrinsic interest and provides a powerful tool to gain insight into magnetic coupling mechanisms [1, 2]. Experimentally, however, access to fluctuations is frequently challenging, owing to two reasons: Firstly, fluctuations can extend over an excessively large range of frequencies. Secondly, many relevant magnetic systems are small entities with dimensions in the nanometer range, such as single molecules, clusters, or magnetic domains. Hence, the study of magnetic fluctuations requires a measurement technique featuring simultaneously nanoscale resolution and a wide frequency bandwidth.

Widely used methods to study ensembles of magnetic nanosystems are SQUID magnetometry [3, 4], Mößbauer spectroscopy [5], electron spin resonance [6], neutron scattering [7], or X-ray magnetic circular dichroism [8]. Furthermore, individual magnetic nano-objects have been investigated by scanning probe microscopy [9, 10], micro-SQUIDs [11, 12] or scanning X-ray microscopy [13]. In general these techniques have a limited detection bandwidth, such that the experimental observation of magnetic fluctuations in a wide frequency range relies on stitched measurements combining complementary techniques in different frequency domains.

Here we show that the Nitrogen-Vacancy (NV) center in diamond employed as a magnetic field sensor [14, 15] simultaneously provides access to both nanoscale objects and a frequency bandwidth spanning ten orders of magnitude. We use the unique properties of the NV to monitor thermal magnetization reversals of single biological nano-magnets from cryogenic to room temperature where these fluctuations accelerate from the sub-Hz to the GHz range.

We study ferritin protein complexes adsorbed onto a diamond surface (Fig. 1a). Each of these proteins en-

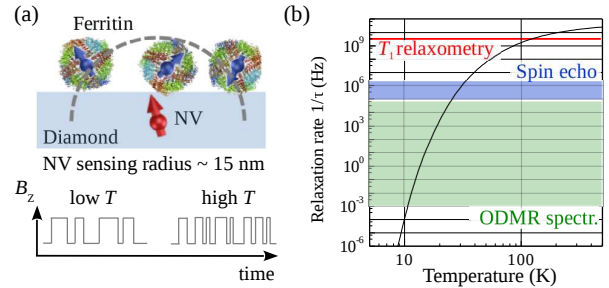


FIG. 1. (a) Ferritin molecules adsorbed to the diamond surface couple to shallow implanted NV centers. The magnetization reversals of the ferritin generate magnetic telegraph noise with a temperature dependent fluctuation rate. (b) Ferritin relaxation rate as a function of temperature for  $E_a = 29$  meV. The sensitivity ranges of different detection protocols for NV magnetometry are indicated.

closes a cluster of up to 4500 Fe atoms with net magnetic moment exhibits strong thermally activated fluctuations. We detect the magnetic stray field of these clusters with NV defect centers embedded 5–10 nm below the diamond surface. This center enables the precise determination of the local magnetic field via the Zeeman shift of its spin sublevels, which can be measured by optically detected magnetic resonance (ODMR) techniques. Due to its atomic size, an individual NV center can be placed as sensor spin in nanometer proximity to the sample [15, 16], allowing for coupling to only a single ferritin complex. Moreover, it can sense magnetic field fluctuations on various frequency scales from the sub-Hz [17] over the kHz–MHz [18, 19] to the GHz range [20], depending on the spectroscopy protocol employed. As a notable extension of previous studies, we here demonstrate nanosensing in a variable temperature setup between 5–300 K in ultrahigh vacuum [21].

Over this temperature range, magnetic fluctuations of ferritin cores exhibit a rich variety of dynamic phenomena like superparamagnetism [22], superantiferromagnetism [4], and macroscopic quantum tunneling [3]. The Fe atoms in the biomineral core are stored in form of a hydrous ferric oxide-phosphate mineral similar in structure to ferrihydrate [23]. At lower temperatures the  $\text{Fe}^{3+}$  spins are antiferromagnetically coupled with a Néel temperature estimated to be between 240 K [23] and 500 K [4]. In the antiferromagnetic phase, the ferritin core possesses a net magnetic moment on the order of  $300\mu_B$  due to an imperfect compensation of the  $\text{Fe}^{3+}$  spins on the two sublattices [5, 24]. The core is generally considered as single magnetic domain with uniaxial anisotropy, therefore the magnetic moment fluctuates thermally activated between two easy directions with a temperature dependent rate. The dynamic of these stochastic magnetization reversals is characterized by the spin lifetime

$$\tau(T, E_a) = \tau_0 \cdot \exp(E_a/k_B T) \quad (1)$$

with the inverse attempt frequency  $\tau_0 \approx 2 \times 10^{-11}$  s [7] and the anisotropy barrier  $E_a$ . This anisotropy barrier is dominated by the magnetocrystalline energy [5]. The magnetization reversals of an individual molecule with the temperature dependent relaxation rate  $1/\tau$  (Fig. 1b) generates magnetic field fluctuations resembling random telegraph noise. The normalized spectral density of this spin noise is calculated to [20]

$$S(\omega, T, E_a) = \frac{2}{\pi} \frac{\tau(T, E_a)}{1 + \tau(T, E_a)^2 \omega^2}. \quad (2)$$

With lower temperatures the cut-off frequency of  $S(\omega, T, E_a)$  decreases, while the low frequency amplitude increases (Fig. 2). To account for the spread of  $E_a$  in the measured ferritin ensembles we assume a log-normal distribution function [25].

Our method to detect these fluctuations is based on changes in the longitudinal ( $T_1$ ) or transverse ( $T_2, T_2^*$ ) [26] spin relaxation time of the NV center in response to the ferritin spin noise. The relaxation rate of the NV center can be written in general as

$$\frac{1}{T_i} = \left( \frac{1}{T_i} \right)_{\text{int}} + \int \langle B^2 \rangle \cdot S(\omega, T, E_a) \cdot F_i(\omega) d\omega, \quad (3)$$

where  $(T_i^{-1})_{\text{int}}$  accounts for intrinsic relaxation mechanisms and  $\sqrt{\langle B^2 \rangle}$  is the effective magnetic field at the NV position generated by the magnetic ferritin core, corresponding to the distance-dependent dipolar coupling strength. In this equation the spectral response function  $F_i(\omega)$  depends on the employed sensing protocol. To access different frequency ranges, we probe the relaxation of the NV center by the inversion recovery protocol [27], spin echo spectroscopy [28], and ODMR-spectroscopy [17]. The corresponding response functions and spectral

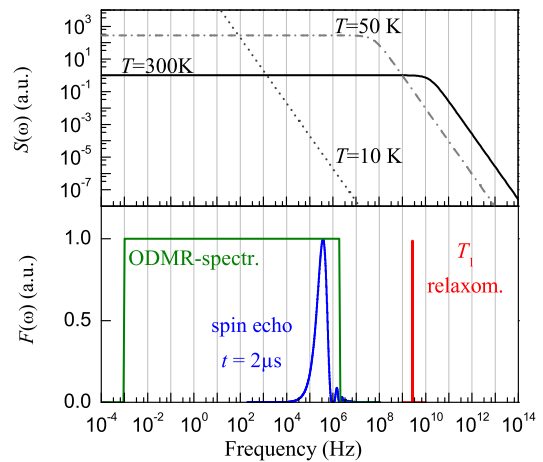


FIG. 2. Spectral density  $S(\omega)$  of the ferritin spin noise at different temperatures for an anisotropy barrier of  $E_a = 25$  meV. The filter functions  $F(\omega)$  of  $T_1$  relaxometry, spin echo spectroscopy and ODMR-spectroscopy are depicted below.

Technique	Filterfunction $F_i(\omega)$	Frequency range
$T_1$ relaxom.	$\frac{1}{\pi} \frac{\Gamma}{\Gamma^2 + (\omega - \omega_L)^2}$	$\sim 3$ GHz
Spin echo	$\frac{1}{t} \left  \frac{\sin^2(\omega t/4)}{\omega/4} \right ^2$	0.1–1 MHz
ODMR spectr.	$\begin{cases} \frac{1}{c}, & \frac{2\pi}{t_{acq}} < \omega < \frac{2\pi}{t_\pi} \\ 0, & \text{else} \end{cases}$	$10^{-3}$ – $10^6$ Hz

TABLE I. Filter functions  $F(\omega)$  and corresponding frequency ranges for the employed detection protocols.  $\Gamma = 1/T_2^*$ : NV dephasing rate,  $\omega_L$ : NV transition frequency,  $t$ : free evolution time,  $c$ : normalization constant,  $t_{acq}$ : acquisition time,  $t_\pi$ : microwave pulse length.

sensitivity ranges are summarized in table I and Fig. 2. For ODMR spectroscopy, which was carried out by applying a single microwave pulse with varying frequency, we assumed a constant sensitivity in a frequency window limited by the averaging time per spectrum  $t_{avg} = 10^3$  s and the length of the microwave pulse  $t_\pi = 500$  ns.

With decreasing temperature the ferritin noise spectrum is subsequently shifted through these distinct sensitivity windows which we verify by measurements on an ensemble of ferritin molecules (Fig. 3). Without adsorbed ferritin we measure  $T_1 = 0.67 \pm 0.15$  ms at  $T = 300$  K which increases to  $> 2.5$  ms at low temperature, i. e. above the longest decay time detectable in our setup. Upon the adsorption of ferritin molecules, the  $T_1$  time at room temperature is reduced by approximately a factor of 5, which has been previously observed for bulk diamonds [29] and diamond nanocrystals [30]. The ferritin-induced reduction in  $T_1$  vanishes at low temperatures, since the cut-off frequency of the ferritin noise spectrum

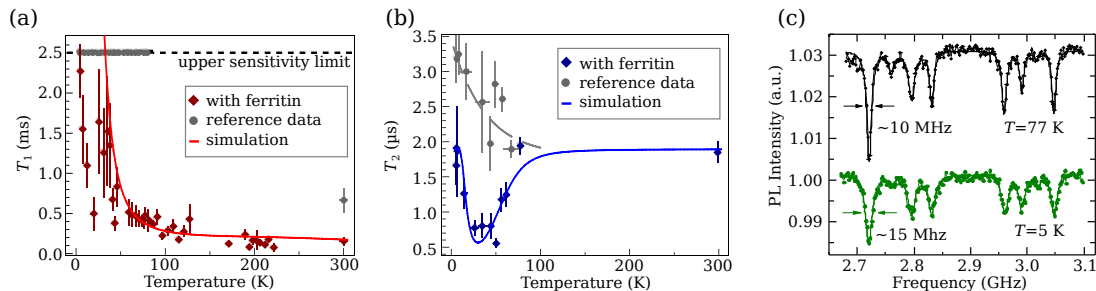


FIG. 3. Measurements on NV ensembles interacting with ferritin molecules. (a) Longitudinal relaxation time  $T_1$  (diamonds), and simulation using  $\overline{E_a} = 15$  meV and  $\sqrt{\langle B^2 \rangle} = 22$  MHz (full line). The longest detectable decay time of 2.5 ms is indicated as upper sensitivity limit by the dashed line. (b) Spin coherence time  $T_2$  (diamonds), and simulation using  $\overline{E_a} = 25$  meV and  $\sqrt{\langle B^2 \rangle} = 10$  MHz (full line). Reference data without ferritin in (a) and (b) are shown as circles. (c) ODMR spectra acquired at 5 K and 77 K.

shifts below the NV transition frequency. In the low temperature regime ( $k_B T \ll E_a$ ) the ferritin magnetization is static on the timescale of the measurement, since magnetization reversals over the energy barrier are suppressed. The data show thus a strong increase in  $T_1$  below the blocking temperature of  $T_B \approx 50$  K. Assuming a temperature dependent intrinsic relaxation rate as found in reference [27], we can well describe the measurement within our model with the fit-parameters  $\overline{E_a} \approx 15$  meV and  $\sqrt{\langle B^2 \rangle} = 22$  MHz [31].

To probe the temperature dependence of the ferritin magnetization dynamics in the range 0.1–1 MHz we employ spin echo spectroscopy. The coherence time  $T_2$  time is rather unaffected by the ferritin spin noise at 300 K, due to the low noise amplitude in the probed frequency range (Fig. 3b). The intrinsic relaxation rate is comparably high due to the surface proximity of the NV centers [32]. This changes at low temperatures; as the cut-off frequency of the ferritin noise spectrum decreases, the noise amplitude in the probed frequency range initially increases. The ferritin contribution to the relaxation rate becomes dominant for  $T \lesssim 80$  K, leading to a reduction of  $T_2$ . At  $T \lesssim 35$  K, the cut-off frequency of the ferritin noise spectrum shifts below the detection window of the spin echo sequence, resulting in a recovery of the  $T_2$  time. The minimum in  $T_2$  at roughly 35 K corresponds to the blocking temperature for the probed frequency range. The reference measurement acquired without adsorbed ferritin shows only a modest increase of  $T_2$  with lower temperature, which might be related to temperature dependent intrinsic relaxation processes. We reach an overall good agreement when fitting the data with the above described model, yielding  $\overline{E_a} = 25$  meV and  $\sqrt{\langle B^2 \rangle} = 10$  MHz.

The deviation in  $\overline{E_a}$  and  $\sqrt{\langle B^2 \rangle}$  between the  $T_1$  and  $T_2$  measurement can be rationalized by the fact that different samples were used, and correspondingly the distribution of anisotropy barriers and the number of detected molecules were different in both experiments. In general

the obtained values correspond well to reported average anisotropy barriers in ferritin of  $\sim 28$  meV determined by Mößbauer spectroscopy and magnetization measurements [25, 33].

We obtain further insight into the ferritin spin dynamics especially at low frequencies by ODMR spectroscopy at  $T = 77$  K and 5 K (Fig. 3c). At 5 K we detect an increase of the resonance line width by roughly 5 MHz, which can be attributed to inhomogeneous broadening [6]. At 77 K the majority of the ferritin molecules fluctuate with a rate faster than the inverse microwave pulse length (500 ns), such that only the average magnetization of the molecular ensemble is detected. At 5 K the spin dynamics of most molecules is blocked, therefore the magnetization is static over the measurement time ( $\sim 10^3$  s) and the local magnetic field differs for each NV center depending on the size and the orientation of the nearby molecules. The low temperature line width of  $\sim 15$  MHz is comparable to the coupling strength  $\sqrt{\langle B^2 \rangle}$  estimated from the  $T_1$  and  $T_2$  measurements. This corresponds to an effective internal field in the NV center ensemble of  $\sim 500$   $\mu$ T which is consistent with the expected stray field of ferritin molecules ( $\mu \approx 300 \mu_B$ ) on the diamond surface.

The obtained blocking temperatures can be compared to values reported for horse-spleen ferritin using other detection techniques; susceptibility measurements (characteristic measurement time  $\tau_m \sim 10^{-3}$ – $10^2$  s) yield blocking temperatures in the range 5–20 K [3, 5, 24, 33], Mößbauer spectroscopy ( $\tau_m \sim 10^{-8}$  s) 30–50 K [5, 22, 23], and electron spin resonance spectroscopy ( $\tau_m \sim 10^{-10}$  s)  $\sim 100$  K [6]. Our findings using NV magnetometry are thus consistent with previously reported results. Furthermore, we point out that NV magnetometry can cover a significantly wider frequency range than the above mentioned techniques and that by using different detection protocols or applying magnetic fields the spectral sensitivity can be further extended.

An important advantage of the NV sensor is the ex-

tremely high sensitivity with the potential for the investigation of single molecules [15, 16]. To utilize this capability we reduced the coverage of the adsorbed ferritin such that isolated molecules are obtained. By employing individual NV centers as sensors, the number of detected molecules can be expected to be very low due to the short range interaction. We studied the same NV centers ( $\sim 35$  in total) before and after ferritin deposition and found for roughly 50% a pronounced reduction of  $T_1$  at room temperature. These centers interacting with only one or a few molecules were investigated at variable temperature.

Figure 4a shows the coherence time  $T_2$  for a representative single NV center revealing several minima. Measurements on other NV centers yield similar curves with one or multiple minima with a rather small width. The dips in  $T_2$  fall in the same temperature range as the broad feature observed in the ensemble measurements (Fig. 3b). To model the response of the NV center to a single molecule we use  $S(\omega)$  without ensemble broadening and found a good agreement to the observed minimum in  $T_2$  at  $T = 47$  K using  $E_a = 43$  meV and  $\sqrt{\langle B^2 \rangle} = 1.5$  MHz (Fig. 4b). The width of the simulated minimum is on the order of 10 K, which corresponds well to the sharp features observed in the experiment. These findings support the interpretation that the observed minima are the fingerprint of individual molecules with different blocking temperatures in the vicinity of the NV center. This technique enables thus the determination of anisotropy barriers on the single molecule level.

The low temperature resonance line width in the ODMR spectra of single NV centers depends on the anisotropy barrier of the nearby molecules. We observe a broadening at 5 K for roughly 20% of the investigated NV centers (Fig. 4c) which we attribute to the magnetic fluctuations of molecules with rather low anisotropy energy such that  $T_B < 5$  K. In contrast, most NV centers show similar line shapes at 5 K and 77 K (Fig. 4d), indicating that nearby molecules are blocked at 5 K. The simulated NV decoherence time  $T_2^* \propto \Gamma^{-1}$  (Fig. 4e) suggests that the low temperature broadening of the linewidth  $\Gamma$  is related to molecules with  $E_a < 15$  meV, which is consistent with the expected spread of anisotropy energies in the sample [25].

The static magnetization of the blocked ferritin molecules is expected to result in a random shift of the transition frequency between 5 K and 77 K. Experimentally we find this shift to be  $\sim 1$  MHz for all NV centers studied, which is significantly smaller than the line broadening of  $\sim 5$  MHz observed for the unblocked molecules (Fig. 4c). This deviation in the coupling strength might be related to the existence of a second magnetic phase located at the particle surface [6, 34], which aligns anti-parallel to the interior of the core at low temperature and thus reduces the net magnetic moment.

In conclusion, we demonstrated the detection of the

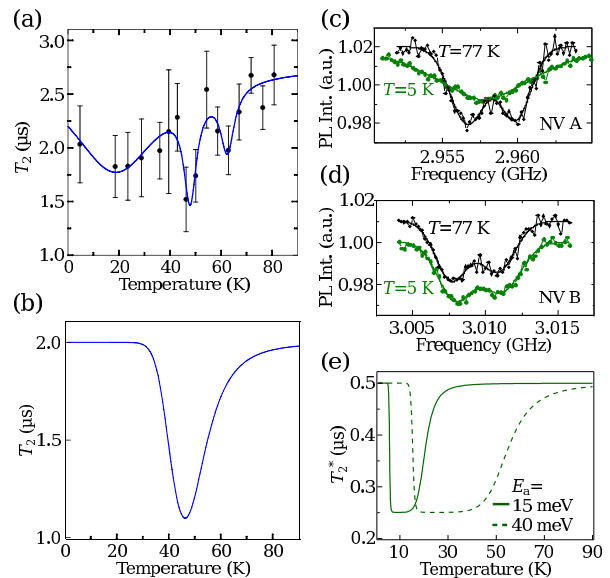


FIG. 4. (a) Temperature dependent  $T_2$  of a single NV center interacting with isolated molecules. (b) Simulated  $T_2$  for a NV center coupling to a single molecule with  $E_a = 43$  meV and  $\sqrt{\langle B^2 \rangle} = 1.5$  MHz. (c) and (d): Representative ODMR spectra of single NV centers. Low temperature line broadening as shown in (a) was observed for  $\sim 20\%$  of the investigated NV centers. (e) Calculated temperature dependence of  $T_2^*$  for an NV center coupling to ferritin molecules with large ( $E_a = 40$  meV, full line) and small ( $E_a = 15$  meV, dashed line) anisotropy barrier.

temperature dependent relaxation dynamics of ferritin molecules by employing NV magnetometry. The main advantages of this approach are the wide frequency range that can be covered and the extremely high sensitivity enabling single molecule experiments. While in the single NV center experiments demonstrated here the number of detected ferritin molecules could only be estimated, future experiments using NV spin sensors in a scanning probe architecture [21, 35, 36] will facilitate single molecule investigations with enhanced control and precision. Due to its high sensitivity and its intrinsic spatial resolution the technique can also be applied to investigate systems with smaller magnetic moment, such as molecular magnets, radicals, or, ultimately nuclear spins.

F.R. and J.W. acknowledge financial support by the EU (SquTec, Diadems), Darpa (Quasar), BMBF (CHISTERA) and contract research of the Baden-Württemberg foundation.

\* m.ternes@fkf.mpg.de

- [1] P. A. Lee, N. Nagaosa, and X. G. Wen, Rev. Mod. Phys. **78**, 17 (2006).
- [2] W. T. Coffey and Y. P. Kalmykov, J. Appl. Phys. **112**, 121301 (2012).

- [3] S. Gider, D. D. Awschalom, T. Douglas, S. Mann, and M. Chaparala, *Science* **268**, 77 (1995).
- [4] C. Gilles, P. Bonville, H. Rakoto, J. M. Broto, K. K. W. Wong, and S. Mann, *J. Mag. Mag. Mat.* **241**, 430 (2002).
- [5] G. C. Papaefthymiou, *Biochim. Biophys. Acta* **1800**, 886 (2010).
- [6] E. Wajnberg, L. J. El-Jaick, M. P. Linhares, and D. M. S. Esquivel, *J. Mag. Res.* **153**, 69 (2001).
- [7] S. Mørup, D. E. Madsen, C. Frandsen, C. R. H. Bahl, and M. F. Hansen, *J. Phys.: Condens. Matter* **19**, 213202 (2007).
- [8] P. Gambardella, S. Rusponi, M. Veronese, S. S. Dhesi, C. Grazioli, A. Dallmayer, I. Cabria, R. Zeller, P. H. Dederichs, K. Kern, C. Carbone, and H. Brune, *Science* **300**, 1130 (2003).
- [9] S. Loth, S. Baumann, C. P. Lutz, D. M. Eigler, and A. J. Heinrich, *Science* **335**, 196 (2012).
- [10] A. A. Khajetoorians, B. Baxevanis, C. Hübner, T. Schlenk, S. Krause, T. O. Wehling, S. Lounis, A. Lichtenstein, D. Pfannkuche, J. Wiebe, and R. Wiesendanger, *Science* **339**, 55 (2013).
- [11] W. Wernsdorfer, *Nature Materials* **6**, 174 (2007).
- [12] P. F. Vohralik and S. K. H. Lam, *Supercond. Sci. Technol.* **22**, 064007 (2009).
- [13] A. Balan, P. M. Derlet, A. F. Rodriguez, J. Bansmann, R. Yanes, U. Nowak, A. Kleibert, and F. Nolting, *Phys. Rev. Lett.* **112**, 107201 (2014).
- [14] A. Gruber, Dräbenstedt, C. Tietz, L. Fleury, J. Wrachtrup, and Borczykowski, *Science* **276**, 2012 (1997).
- [15] J. M. Taylor, P. Cappellaro, L. Childress, L. Jiang, D. Budker, P. R. Hemmer, A. Yacoby, R. Walsworth, and M. D. Lukin, *Nature Physics* **4**, 810 (2008).
- [16] C. L. Degen, *Nature Nanotechnology* **3**, 643 (2008).
- [17] A. Dréau, M. Lesik, L. Rondin, P. Spinicelli, O. Arcizet, J.-F. Roch, and V. Jacques, *Phys. Rev. B* **84**, 195204 (2011).
- [18] T. Staudacher, F. Shi, S. Pezzagna, J. Meijer, J. Du, C. A. Meriles, F. Reinhard, and J. Wrachtrup, *Science* **339**, 561 (2013).
- [19] H. J. Mamin, M. Kim, M. H. Sherwood, C. T. Rettner, K. Ohno, D. D. Awschalom, and D. Rugar, *Science* **339**, 557 (2013).
- [20] S. Steinert, F. Ziem, L. T. Hall, A. Zappe, M. Schweikert, N. Götz, A. Aird, G. Balasubramanian, L. Hollenberg, and J. Wrachtrup, *Nature Comm.* **4**, 1607 (2013).
- [21] E. Schaefer-Nolte, F. Reinhard, M. Ternes, J. Wrachtrup, and K. Kern, *Rev. Sci. Instr.* **85**, 013701 (2014).
- [22] R. B. Frankel, G. C. Papaefthymiou, and G. D. Watt, *Hyperfine Interact.* **66**, 71 (1991).
- [23] E. R. Bauminger and I. Nowik, *Hyperfine Interact.* **50**, 489 (1989).
- [24] J. G. E. Harris, J. E. Grimaldi, and D. D. Awschalom, *Phys. Rev. B* **60**, 3453 (1999).
- [25] D. E. Madsen, M. F. Hansen, J. Bendix, and S. Mørup, *Nanotechnology* **19**, 315712 (2008).
- [26]  $T_2^*$  is the spin decoherence time affected mainly by low-frequency noise compared to  $T_2 > T_2^*$  which is only sensitive to noise in the detection window at higher frequency.
- [27] A. Jarmola, V. M. Acosta, K. Jensen, S. Chemerisov, and D. Budker, *Phys. Rev. Lett.* **108**, 197601 (2012).
- [28] A. Laraoui, J. S. Hodges, and C. A. Meriles, *Appl. Phys. Lett.* **97**, 143104 (2010).
- [29] F. Ziem, N. S. Götz, A. Zappe, S. Steinert, and J. Wrachtrup, *Nano Lett.* **13**, 4093 (2013).
- [30] A. Ermakova, G. Pramanik, J.-M. Cai, G. Algara-Siller, U. Kaiser, T. Weil, Y.-K. Tzeng, H.-C. Chang, L. P. McGuinness, M. B. Plenio, B. Naydenov, and F. Jelezko, *Nano Lett.* **13**, 3305 (2013).
- [31] The effective magnetic field as a measure of coupling strength is given in frequency units for a gyromagnetic ratio  $\gamma = 28$  MHz/mT.
- [32] T. Rosskopf, A. Dussaux, K. Ohashi, M. Loretz, R. Schirhagl, H. Watanabe, S. Shikata, H. Itoh, and C. L. Degen, *Phys. Rev. Lett.* **112**, 147602 (2014).
- [33] S. H. Kilcoyne and R. Cywinski, *J. Mag. Mag. Mat.* **144**, 1466 (1995).
- [34] R. A. Brooks, J. Vymazal, D. Goldfarb, J. W. M. Bulte, and P. Aisen, *Magn. Reson. Med.* **40**, 227 (1998).
- [35] P. Maletinsky, S. Hong, M. S. Grinolds, B. Hausmann, M. D. Lukin, R. Walsworth, M. Loncar, and A. Yacoby, *Nature Nanotechnology* **7**, 320 (2012).
- [36] L. Rondin, J.-P. Tetienne, P. Spinicelli, C. Dal Savio, K. Karrai, G. Dantelle, A. Thiaville, S. Rohart, J.-F. Roch, and V. Jacques, *Appl. Phys. Lett.* **100**, 153118 (2012).